Silicon Nanowires

DOI: 10.1002/anie.200902451

Directionally Integrated VLS Nanowire Growth in a Local Temperature Gradient**

*Geunhee Lee, Yun Sung Woo, Jee-Eun Yang, Donghun Lee, Cheol-Joo Kim, and Moon-Ho Jo**

Integrated nanowire (NW) ensembles can be used in various applications in electronic circuits, biological probes, and energy conversion systems.[1–5] The self-organization of nanowires requires spontaneous ordering over a large anisotropic energy barrier set at the different length scales in the axial and radial directions. Herein, we report a simple and robust growth mechanism that coherently directs the nanowire growth directions by introducing a local temperature gradient as the local kinetic variable during the conventional vapor–liquid–solid (VLS) growth. This NW growth, which is the earliest and prevailing synthetic route for semiconductor NWs, typically occurs in spatially uniform heating zones that surround the growing crystals on substrates; thus, all the reactions for NW growth at the VLS phase boundaries are isothermal.[6–8] The differences in the chemical potentials of the growth species are the thermodynamic driving force for the VLS growth, which occurs uniformly along the VLS interfaces, through which the growth species diffuse.[9] The crystallographic orientation of a NW is thermodynamically determined at the LS interface within the eutectic liquid droplet of given size and geometry during the initial nucleation.[10,11] Nevertheless, the embryonic NWs nucleate in an isotropically random manner at the edges of the hemispheric droplets,[12,13] thus leading to an unpredictable growth direction, unless external constraints such as directional epitaxy[14,15] and guiding templates are imposed.[11] Consequently, the systematic integration of VLS NWs usually requires supplementary processes after the NW growth.[16–21] In principle, however, any local variation in the interfacial thermodynamics, that is, local temperature variations at the interfaces, can influence the elemental growth behavior. In our growth scheme, we imposed a temperature gradient normal to the substrate plane during the VLS Si NW growth, and observed that the NW growth parallel to the local temperature gradient is spontaneous and directional, with a significantly increased growth rate compared to the isothermal growth. We also provide a phenomenological model for the directional NW growth within the framework of the interfacial thermodynamic stability. In particular, we discuss the role of the temperature gradient on the redistribution of a local kinetic variable, that is, local interfacial supersaturation, on the thermodynamic stability at the fluctuating VL and LS interfaces. Our growth scheme provides practical implication for the growth of integrated NW ensembles.

The design of our VLS chemical vapor reactor (Figure 1a), is much the same as the conventional hot-wall tube furnace,[22,23] except that the susceptor underneath the growth substrates can be cooled by air circulation (Figure S1 in the Supporting information). One can thus expect that the VLS growth is not isothermal, and instead that a stable temperature gradient is established perpendicular to the substrate. For example, when the reactor wall is heated at 650 °C by the furnace, the substrate temperature is maintained at 490 °C under air cooling. Figure 1b shows the simulated temperature distribution within the reactor.

We wish to emphasize two aspects of our main observations. Firstly, the Si NW growth directions are vertical over the large areas (region A in Figure 1c). This observation is consistent with the direction of the temperature gradient. Secondly, the axial growth rate is unprecedentedly enhanced compared to the isothermal growth (see also Figure 3). The tendency to vertically aligned NW growth is found regardless of the types of substrates or the catalyst density, as similar behavior is observed on quartz, indium tin oxide, and alumina substrates (Figure S2 in the Supporting Information). Apparently, the growth direction is not dictated by possible epitaxial relations with crystalline substrates. Moreover, when Si NWs are grown on the edge of the substrate, over which the temperature gradient is radially distributed, (Figure 1c, region B), the NW growth direction precisely follows the temperature gradients at all different positions along the edge. The length of the NW growth is proportional to the magnitude of the temperature gradients, which increase with the proximity of lateral position to the edge (Figure 1d). These observations unequivocally demonstrate that the NW growth velocity, that is, its direction and magnitude, follows the local temperature gradient.

We found two additional features by examining the individual NWs along the entire length from the bottom to top, as in the time-lapse SEM images (Figure 2a–e). In the very early growth stage (Figure 2a,b), the individual NWs

[*] Dr. G. Lee, Dr. Y. S. Woo, J.-E. Yang, D. Lee, C.-J. Kim, Prof. M.-H. Jo
Department of Materials Science and Engineering
Pohang University of Science and Technology (POSTECH)
San 31, Hyoja-Dong, Nam Gu, Pohang, Gyungbuk 790-784 (Korea)
Fax: (+82) 54-279-2399
E-mail: mhjo@postech.ac.kr
Homepage: http://www.postech.ac.kr/lab/mse/ndmpl/
Prof. M.-H. Jo
Graduate Institute of Advanced Materials Science
Pohang University of Science and Technology (POSTECH)
San 31, Hyoja-Dong, Nam Gu, Pohang, Gyungbuk 790-784 (Korea)

[**] We thank Prof. Byeong-Joo Lee for helpful discussions on the thermodynamics of nanowire growth. This work was supported by the Nano R&D program through the NRF (2007-02864), "System IC 2010" of the MEST, the MEST-AFOSR NBIT, the KRF Grant MOEHRD (KRF-2005-005J13103), and the WCU program through by MEST (R31-2008-000-10059-0). VLS = vapor–liquid–solid.

Supporting information for this article is available on the WWW under http://dx.doi.org/10.1002/anie.200902451.

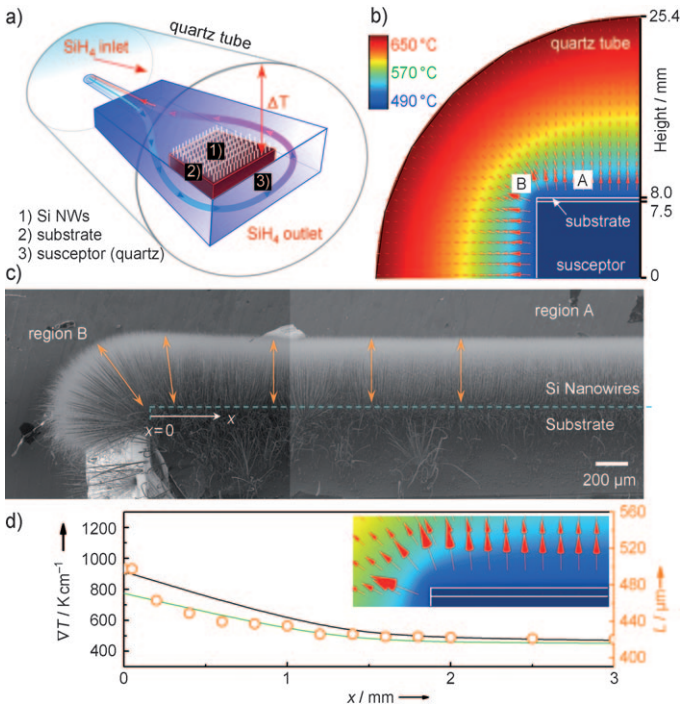

Figure 1. a) Illustration of the VLS reactor used in this study. b) Three-dimensional computational simulation of the temperature profile (filled colors) and its gradient (arrows) within the reactor for the Si NW growth on SiO_2/Si substrates using 10% of SiH_4 premixed in He as the vapor precursors. c) Cross-sectional scanning electron microscopy (SEM) view of Si NWs grown at regions A and B in (b) for 46 min. d) The measured NW length (*l*, open circle) and the simulated temperature gradient (∇T, above 10 μm (black line) and 100 μm (green line) from the substrate) along the position of substrate from an edge. The inset shows a magnification of the temperature profile and its gradient near region B in (b).

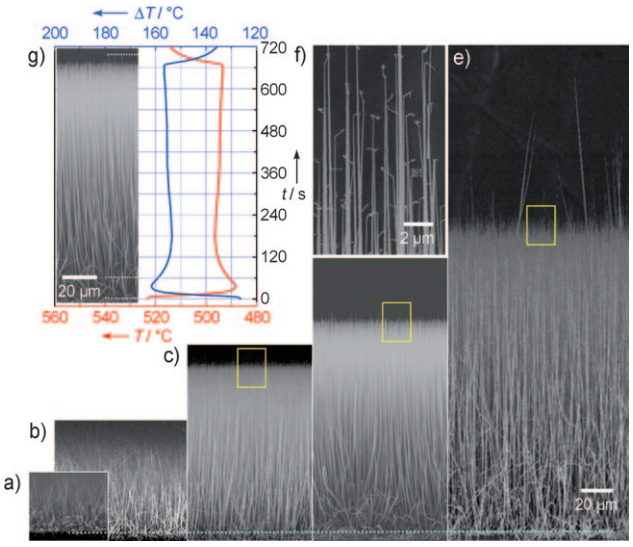

Figure 2. SEM views of Si NWs grown for a) 3.5 min, b) 6 min, c) 8.5 min, d) 11 min, and e) 16 min. f) Magnified view of the kinks near the catalytic tips as observed in the yellow rectangle in (c)–(e). g) Temperature of the substrate (*T*, red line) and the temperature difference between the substrate and the furnace wall (ΔT, blue line) with growth time (*t*). The inset shows the NWs grown in the corresponding growth time.

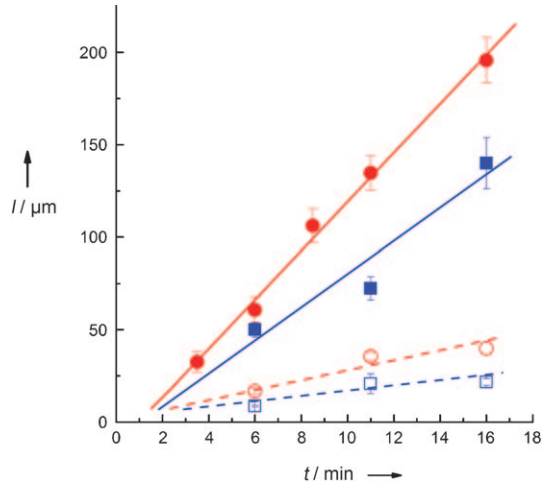

Figure 3. The measured NW length (*l*) as a function of growth time (*t*) with temperature gradient (solid red symbols) and with the isothermal growth at 490 °C (open red symbols) using SiH_4 diluted in He. The similar data collected using SiH_4 diluted in H_2 (solid and open blue rectangles).

point in random directions, but subsequently they grow in a straight vertical direction (Figure 2c–e). In addition, as seen in Figure 2f, we observed reproducible unique kinks near the catalytic tips (yellow boxes in Figure 2c–e). For instance, out of the 146 NWs counted in Figure 2e, we found that 144 NWs exhibited abrupt kinks near the NW tips. We attribute this local nonlinearity during the very early and final growth stages to the variation of the substrate temperature that inevitably arises from the temperature gradient in our growth sequences. As shown in Figure 2g, when the cold SiH_4 vapor was initially introduced into the reactor with a temperature gradient, the substrate temperature decreased during the initial 3.5 minutes. The substrate temperature then remained at 495 °C in a steady flow of the vapor precursor. Notably, the time sequence of the initial curvature of the NWs corresponds to the initial temperature decrease, hence the finite incubation time for the stable temperature gradient (Figure S3b in the Supporting Information). As mentioned above, the NW growth direction in the stable temperature gradient is straight. During the pumping out of the vapor precursor in order to stop the growth in the last sequence, a residual NW growth from depleting vapor precursors still occurred. The concomitant rapid temperature increase may be responsible for the kinks near the tip. This observation is reminiscent of an earlier report in which the morphological stability upon the temperature change, such as the configuration of the wetting angles of the eutectic liquid droplets at the LS interface, was attributed to the formation of kinks and branches during the VLS growth of Si whiskers.[24,25] All the aforementioned observations unanimously support the conclusion that the directional NW growth is consistent along the temperature gradient, and any deviation in stability of the temperature gradient is responsible for the random directional growth.

The presence of the temperature gradient during the VLS growth is also manifested in the axial NW growth kinetics. We have observed that the axial growth rate is an order of magnitude greater than the isothermal NW growth at 490 °C (Figure 3). For comparison, we carried out further control experiments of the Si NW growth in an identical temperature gradient using SiH_4 diluted in H_2 instead of He. We found that the axial growth rate under the temperature gradient was also enhanced severalfold compared to that of the isothermal growth, although the rates are less than those of growth using SiH_4 diluted in He. Nevertheless, we have not observed any directional growth using SiH_4 premixed in H_2 in the temperature gradient under any growth conditions (Figure S4 in the Supporting Information).

Based on our observations, we provide a phenomenological model of the roles of the temperature gradient by re-examining the VLS process at the VL and LS interfaces, as represented in Figure 4 a–c. The prime driving force for the VLS growth is supersaturation, that is, the differences in the chemical potentials μ of the growth species in the VLS phases, such as $\Delta\mu_{LV}=\mu_V-\mu_L$ and $\Delta\mu_{SL}=\mu_L-\mu_S$.[20,26] It is at the VL interfaces that the axial growth kinetics is controlled.[8,12,27] For example, during the Si VLS NW growth, the dissociative adsorption of SiH_4 vapors on the Au–Si eutectic liquid droplets is recognized as the rate-limiting step.[8] Thus, the presence of the temperature gradient during the VLS growth must manifest itself in the faster catalytic decomposition kinetics of the vapor precursors. The homogeneous decomposition kinetics of SiH_4 in the vapor phase are thermally activated, and are also strongly dependent on the types of the carrier gases, that is, H_2 or He in our study. At the furnace temperature of 650 °C, a significant fraction (mole fraction $\approx$ 80 %) of SiH_4 in He is readily decomposed into more reactant isomers such as SiH_2, even before the precursor arrives at the eutectic liquid catalysts.[26] Thereon, the energy barrier for the dissociative adsorption of SiH_4 into the eutectic droplets is significantly lowered. Furthermore, in comparison with the isothermal growth, the higher vapor concentration can be effectively built up near the colder catalysts by thermal diffusion in the vapor phase along the temperature gradient.[28] Conceptually, this faster decomposition process at the VL interface locally increases the chemical potential in the eutectic liquid (marked as μ_L^* in Figure 4 b), compared to that during the isothermal growth (marked μ_L in Figure 4 a). In the isothermal VLS growth, the crystallographic direction along the NW axis is thermodynamically determined at the LS interfaces during the nucleation stage by interfacial energetics, which are often parameterized as the wetting angle at the three-phase boundary (TPB).[10,11,29] The LS interfaces are usually faceted with a single-crystal plane that is perpendicular to the growth direction. For example, the NW crystallization advances at the LS interfaces by layer-by-layer growth, preferentially nucleated each time from either TPBs,[29] although it often involves the propagation of several atomic layers.[30,31] The conceptual growth velocity v_n is homogeneous and perpendicular to the LS interface (blue arrows in Figure 4 a). However, in the presence of a vertical temperature gradient ∇T, the planar interfacial stability can be perturbed because of the local variation in the interfacial

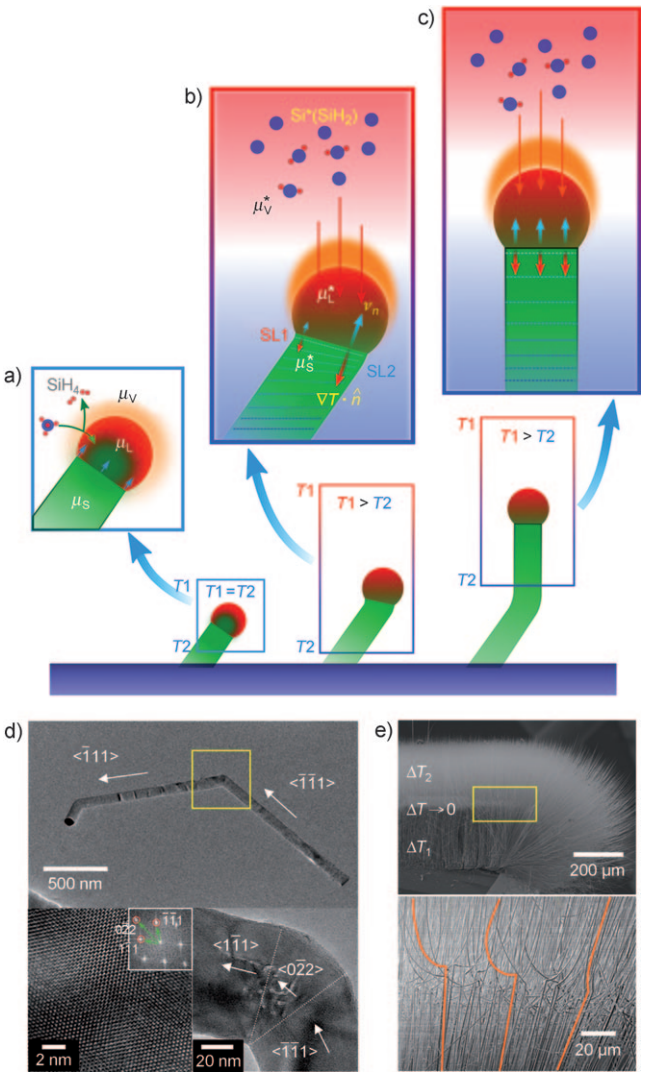

Figure 4. Schematic diagram of a) the isothermal VLS growth of Si NWs, b) VLS-grown Si NWs under the temperature gradient, and c) the vertically VLS-grown Si NW under the temperature gradient in the steady-state growth regime. d) TEM images (upper), diffraction patterns (lower left), and the magnified view of the kink (lower right) marked by the yellow rectangle in the upper panel. e) SEM image (upper) and magnified view (lower) of reversibly direction-guided Si NWs. The kinked regions have orange lines superimposed on them for clarity.

chemical potential in the solid μ_S^* and thus the local $\Delta\mu_{S-L}^*$, which arises from the non-uniform temperature profile. Figure 4 b shows how the interface–normal temperature gradient $\nabla T\cdot\hat{n}$ impressed by the vertical ∇T starts to override the pre-existing thermodynamic interfacial stability, and thus the lower-right edge is subject to a greater $\nabla T\cdot\hat{n}$ (marked by red arrows) that is in turn proportional to the local $\Delta\mu_{SL}^*$. This latter value is now much higher than that in the isothermal growth case, because of the higher $\Delta\mu_L^*$, as discussed above. The nonuniform temperature profile also can break the symmetry of the nucleation kinetics at the opposite TPBs (SL1 and SL2 in Figure 4 b). The combination of these factors can instigate a spatially nonuniform advance

of the LS interface, thus the local v_n is faster (slower) at the lower-right (upper-left) edge, subject to higher (lower) $\Delta\mu^*_{SL}$, until the fluctuating interface become aligned perpendicular to the imposed temperature gradient in another steady-state growth regime (as in Figure 4c). As a macroscopic consequence of this local fluctuation of $\Delta\mu_{SL}$ at the LS interface, the NW growth proceeds by changing its direction to become parallel to the temperature gradient. The observation that the Si NW growth using SiH_4 in H_2 is not directional and has a lower rate than the growth in He is very intriguing. The difference between the vapor precursors in H_2 and He is that only 10% of the precursor decomposes into more reactant isomers for SiH_4 diluted in H_2.[26] This process results in a lower μ_L value for the growth by SiH_4 diluted in H_2; this value may then not be high enough to dictate the growth direction.

It was found that our Si NWs possess the coherent crystallographic orientation such as [111] or [112]along the entire NW length. It is difficult to directly observe any crystallinity variation over the NW directional change using TEM, since the growth direction varies over the significant length over a few micrometers. Nevertheless, possible reasons for the abrupt kinks are provided by Figure 2 f, where the ∇T value must drastically change in the last growth stage. For example, in Figure 4d, the Si NW is initially aligned along the [111] direction, but is temporarily aligned along the [011] direction at the kink and returns to the [111] direction after the kink. While the [111] orientation is thermodynamically stable for Si NWs that are approximately 80 nm thick, the (011) plane stacking is metastable, but can provide a faster growth pathway during the kink formation. We have consistently observed these metastable stacking motifs of the lower packing density planes during the kink formation (Figure S5 in the Supporting Information). Out of more than 40 NWs investigated by TEM, we found the [111]–$[011]_{kink}$–[111] directional change at the kink occurred in 32 NWs and the [112]–$[011]_{kink}$–[112] change occurred in the remaining NWs. This finding suggests that the NW directional change can be kinetically driven over the thermodynamic balance established for the crystallographic orientation. This change is analogous to the kinetically controlled anisotropic growth of colloidal nanocrystals into various nonspherical shapes.[32,33] Indeed, we intermittently turned this kinetic driving force on and off during the NW growth (under ΔT_1) by pausing (thus ΔT approached zero) and resuming (thus ΔT_2 is re-established) the vapor feeding (Figure 4e), and confirmed that the reversible directional guiding of NWs can occur after the complicated kink formation. This result signifies that the VLS NW growth can by kinetically driven by local kinetic manipulation of the interfacial thermodynamic balances.

In summary, we demonstrate a directional VLS NW growth with local kinetic control over the VLS interfaces by imposing a local temperature gradient. In this case, the local temperature gradient as the local kinetic variable is manifested both at the LS and VL interfaces by directional NW growth with fast kinetics.

Experimental Section

Directional nanowire growth: Si NWs were grown in a quartz tube reactor 2 inches in diameter, surrounded by a uniform heating element. The quartz susceptor underneath the growth substrates, which was connected by two inner cores open the atmosphere for air-circulation cooling, was inserted into the quartz tube reactor under the given growth conditions. The typical NW growth was carried out using 10% SiH_4 premixed in He, at a flow rate of 50 sccm at a total pressure of 50 Torr. The nanometer-scale Au catalysts were prepared by deposition of either 2 nm thick Au films or a dispersion of colloidal Au nanoparticles of 20 nm in diameter on SiO_2/Si (100), indium tin oxide, quartz, or alumina substrates. Temperature distribution and gradient in our CVD reactor were estimated by computing the three-dimensional heat transfer model, in which partial differential equations of heat conduction were resolved by the finite element method using COMSOL Multiphysics software.

Received: May 8, 2009
Published online: September 2, 2009

Keywords: interfaces · kinetic control · nanostructures · self-assembly · vapor–liquid–solid growth

[1] W. Lu, C. M. Lieber, *Nat. Mater.* **2007**, *6*, 841–850.
[2] F. Patolsky, B. P. Timko, G. Zheng, C. M. Lieber, *MRS Bull.* **2007**, *32*, 142–149.
[3] C. K. Chan, H. Peng, G. Liu, K. McIlwrath, X. F. Zhang, R. A. Huggins, Y. Cui, *Nat. Nanotechnol.* **2008**, *3*, 31–35.
[4] B. Tian, X. Zheng, T. J. Kempa, Y. Fang, N. Yu, G. Yu, J. Huang, C. M. Lieber, *Nature* **2008**, *449*, 885–890.
[5] M. Law, L. E. Greene, J. C. Johnson, R. Saykally, P. Yang, *Nature Mater.* **2005**, *4*, 455–459.
[6] R. S. Wagner, W. C. Ellis, *Appl. Phys. Lett.* **1964**, *4*, 89–90.
[7] A. M. Morales, C. M. Lieber, *Science* **1998**, *279*, 208–211.
[8] S. Kodambaka, J. Tersoff, M. C. Reuter, F. M. Ross, *Phys. Rev. Lett.* **2006**, *96*, 096105.
[9] B. A. Wacaser, K. A. Dick, J. Johansson, M. T. Borgström, K. Deppert, L. Samuelson, *Adv. Mater.* **2009**, *20*, 153–165.
[10] Y. Wu, Y. Cui, L. Huynh, C. J. Barrelet, D. C. Bell, C. M. Lieber, *Nano Lett.* **2004**, *4*, 433–436..
[11] V. Schmidt, S. Senz, U. Gösele, *Nano Lett.* **2005**, *5*, 931–935.
[12] B. J. Kim, J. Tersoff, S. Kodambaka, M. C. Reuter, E. A. Stach, F. M. Ross, *Science* **2008**, *322*, 1070–1073.
[13] Y. Wu, P. Yang, *J. Am. Chem. Soc.* **2001**, *123*, 3165–3166.
[14] Y. Wang, V. Schmidt, S. Senz, U. Gösele, *Nat. Nanotechnol.* **2006**, *1*, 186–189.
[15] C. J. Kim, D. Lee, H. S. Lee, G. Lee, G. S. Kim, M. H. Jo, *Appl. Phys. Lett.* **2009**, *94*, 173105.
[16] P. J. Pauzauskie, A. Radenovic, E. Trepagnier, H. Shroff, P. Yang, J. Liphardt, *Nature Mater.* **2006**, *5*, 97–101.
[17] S. J. Papadakis, Z. Gu, D. H. Gracias, *Appl. Phys. Lett.* **2006**, *88*, 233118.
[18] G. Yu, A. Cao, C. M. Lieber, *Nat. Nanotechnol.* **2007**, *2*, 372–377.
[19] N. Melosh, A. Boukai, F. Diana, B. Gerardot, A. Badolato, P. Petroff, J. R. Heath, *Science* **2003**, *300*, 112–115.
[20] a) Y. Huang, X. Duan, Q. Wei, C. M. Lieber, *Science* **2001**, *291*, 630–633; b) D. Whang, S. Jin, Y. Wu, C. M. Lieber, *Nano Lett.* **2003**, *3*, 1255–1259; c) A. Javey, S. Nam, R. S. Friedman, H. Yan, C. M. Lieber, *Nano Lett.* **2007**, *7*, 773–777.
[21] J. H. Ahn, H. S. Kim, K. J. Lee, S. Jeon, S. J. Kang, Y. Sun, R. G. Nuzzo, J. A. Rogers, *Science* **2006**, *314*, 1754–1757.
[22] C. B. Jin, J. E. Yang, M. H. Jo, *Appl. Phys. Lett.* **2006**, *88*, 193105.
[23] J. E. Yang, C. B. Jin, C. J. Kim, M. H. Jo, *Nano Lett.* **2006**, *6*, 2679–2684.

[24] R. S. Wagner, C. J. Doherty, *J. Electrochem. Soc.* **1966**, *113*, 1300 – 1305.
[25] R. S. Wagner, C. J. Doherty, *J. Electrochem. Soc.* **1968**, *115*, 93 – 99.
[26] M. E. Coltrin, R. J. Kee, G. H. Evans, *J. Electrochem. Soc.* **1989**, *136*, 819 – 829.
[27] E. I. Givargizov, *J. Cryst. Growth* **1975**, *31*, 20 – 30.
[28] L. J. T. M. Kempers, *J. Chem. Phys.* **2001**, *115*, 6330 – 6341.
[29] F. M. Ross, J. Tersoff, M. C. Reuter, *Phys. Rev. Lett.* **2005**, *95*, 146104.
[30] S. Hofmann, R. Sharma, C. T. Wirth, F. Cervantes-Sodi, C. Ducati, T. Kasama, R. E. Dunin-Borkowski, J. Drucker, P. Bennett, J. Robertson, *Nature Mater.* **2008**, *7*, 372 – 375.
[31] A. I. Persson, M. W. Larsson, S. Stenström, B. J. Ohlsson, L. Samuelson, L. R. Wallenberg, *Nature Mater.* **2004**, *3*, 677 – 681.
[32] X. Peng, L. Manna, W. Yang, J. Wickham, E. Scher, A. Kadavanich, A. P. Alivisatos, *Nature* **2000**, *404*, 59 – 61.
[33] V. F. Puntes, K. M. Krishnan, A. P. Alivisatos, *Science* **2001**, *291*, 2115 – 2117.

